Enhancement of Turbulent Heat Transfer of the Cooling System in Nuclear Reactor by Large Scale Vortex Generation

Kun Ho Chun*, Jong Seuk Park** and Young Don Choi*

Key words: Mixing vane, Spacer grid, Rod bundle, Large scale secondary vortex motion, Turbulent heat transfer

Abstract

Experimental and computational studies were carried out to investigate the turbulent heat transfer enhancement of the cooling system in nuclear reactor by large scale vortex generation. The large scale vortex motion was generated by rearranging the inclination angles of mixing vanes to the coordinate directions. Axial development of mean and turbulent velocities in the subchannels were measured by the 2-color LDV system. Eddy diffusivity concept based on $k-\varepsilon$ model was employed to calculate the turbulent heat and momentum transfers in the subchannel. The turbulences generated by split mixing vanes has small length scales so that they maintain only about $10\,D_H$ after the spacer grid. On the other hand, the turbulences generated by the large scale vortex motions continue longer and remain up to $25\,D_H$ after the spacer gird.

Nomenclature

$C_{\varepsilon 1}, C_{\varepsilon 2}$: Model constants of ε equation
D : Diameter of rod bundle [m]
D_H : Hydraulic diameter [m]
$\sqrt{g}$: Jacobian
$\sqrt{g^{mm}}$: Contravariant matrix tensor
k : Turbulent kinetic energy [m^2/s^2]
P_k : Production rate of k [m^2/s^3]
q : Heat flux [W/m^2]
Re : Reynolds number
T : Temperature [℃]
U, V, W : Cartesian velocities for x, y, z coordinates [m/s]
U^{ξ^m} : Physical contravariant velocity [m/s]
x, y, z : Cartesian coordinate [m]
$\overline{u_i u_j}$: Reynolds stress [$(m/s)^2$]
$\overline{u_i \theta}$: Turbulent heat flux [(m/s)℃]

Greek symbols

α : Angle of mixing vane
β : Pressure drop parameter

* Department of Mechanical Engineering, Korea University, Sungpukku, Seoul 136-701, Korea
** Korea Institute of Nuclear Safety, Yusungku, Taejun 305-338, Korea

γ : Temperature increase parameter

σ_k, σ_ε : Model constants of k and ε equations

ε : Dissipation rate of turbulent kinetic energy [m^2/s^3]

ν : Molecular kinematic viscosity [m^2/s]

ν_t : Eddy viscosity [m^2/s]

ξ^m : General curvilinear coordinate ($m=1, 2, 3$)

1. Introduction

One of the key subjects in nuclear reactor design is to enhance the turbulent thermal efficiency of cooling system. To enhance the turbulent thermal efficiency between rod bundles and coolant flow, split mixing vanes have been attached to the spacer grid of rod bundles to generate the vortex motion.

Rehme[1] published the pressure drop correlation for the applications of the various types of spacer grids. Rehme and Trippe[2] investigated the redistribution phenomena of mass flux through the spacer grid by pitot tube measurement of the velocity distributions. Rowe and Chapman[3] measured the effect of spacer grid on the turbulent structures at the upstream and downstream positions of a spacer grid using LDV. Shen et al.[4] found that the mixing rate mainly depends on the inclination angle of mixing vane attached to the spacer grid. Gu et al.[5] investigated the effects of various types of mixing vanes on the turbulent heat transfer enhancement between rod bundles and coolant flow using FLOW3D computer code. Recently Yang and Chung[6] measured the streamwise velocity, turbulent intensity, skewness factor and flatness factor of the subchannel flow for the 5×5 and 6×6 rod bundles by LDV to find out the effects of spacer grids on the turbulent structures. But all these studies above mentioned consider only the effects of spacer grid and split mixing vane on the turbulent characteristics. The key point in the design of mixing vane is to enhance the thermal efficiency by enhancing the turbulence of the coolant flow. The enhanced turbulence by the attachment of split mixing vanes maintains only to about $10\,D_H$ after spacer grid due to the small length scale of induced turbulence. In consideration of the $55\,D_H$ interval between spacer grids, increasing the turbulence enhanced region is essential to improve the thermal efficiency of nuclear reactor cooling system. Therefore we have attempted to find out the optimal mixing vane shape and arrangement patterns in the subchannel which may extend the turbulence enhancement region most effectively.

Main purpose of the present study is to introduce a new mixing vane pattern, named LSS which is able to improve turbulent thermal efficiency remarkably by extending turbulence enhancement region in comparison with split mixing vane. We compare the measured and predicted streamwise, secondary and turbulent velocities distributions for the subchannels flow of nuclear reactor cooling systems which attach the split and LSS mixing vanes.

2. Experimental approach

Experimental apparatus is composed of a

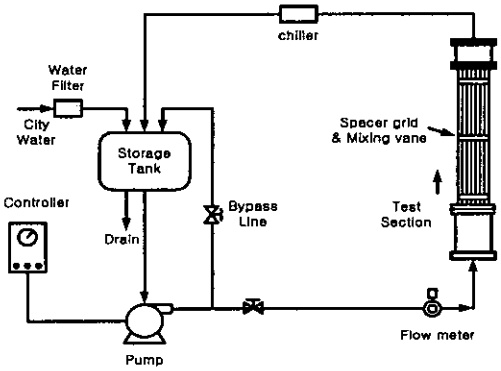

Fig. 1 Test loop and section for the cooling system of nuclear reactor.

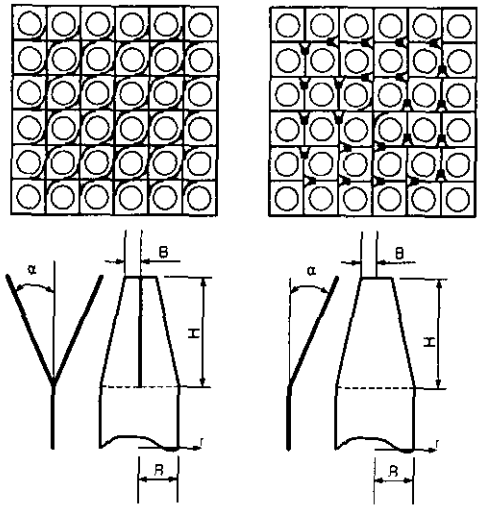

(a) Split mixing vane (b) LSS mixing vane

B(mm)	H(mm)	R(mm)	α (°)
1.5	10.0	3.0	25

Fig. 2 Shape and direction of 6×6 rod bundles, spacer grid and mixing vanes.

water storage tank, pump, chiller, flow control valve, flow meter, and test section as shown in Fig. 1. Spacer grids with mixing vane which hold the 6×6 rod bundle is shown in Fig. 2. The height and cross-section area of the spacer grids are 20 mm and 640 mm^2 with 36 iso-cells. Figure 3 shows the measuring points in streamwise and normal directions of the test section.

Split mixing vanes which have been used frequently in the cooling systems of traditional nuclear reactors induce vortex flows in the subchannel so as to produce strong turbulence. Turbulent kinetic energy generated by LSS mixing vanes decays more slowly than that of split mixing vane because the turbulence are produced from the larger scale vortex motion.

A four-beam two color LDV system was used in the present investigation. The light source is a 300 mW argon ion laser. The focal length of the front lens is 160 mm with a beam separation of 38 mm. The velocity signal was sampled 30,000 data for 20~30 sec. Silicon

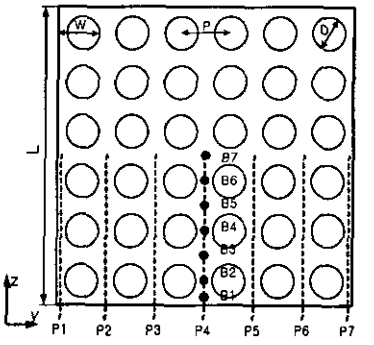

D(mm)	9.5
P(mm)	12.6
W(mm)	9.0
L(mm)	81.0

Fig. 3 Cross-section of 6×6 rod bundle and measurement points and dimension.

carbide particles with 1.5 μm mean diameter are used for seeding purpose.

3. Analysis

3.1 Governing equation

The continuity and momentum equations for the incompressible turbulent flow in the subchannel of nuclear reactor cooling system is written

Continuity equation

$$\frac{1}{\sqrt{g}}\frac{\partial}{\partial \xi^m}(\rho\sqrt{g}\sqrt{g^{mm}}\,U^{\xi^m}) = 0 \tag{1}$$

$$U^{\xi^m} = \frac{1}{\sqrt{g^{mm}}}\left(\frac{\partial \xi^m}{\partial x}U + \frac{\partial \xi^m}{\partial y}V + \frac{\partial \xi^m}{\partial z}W\right) \tag{2}$$

where, $\sqrt{g}$ is Jacobian, g^{mm} is contravariant matrix tensor and U^{ξ^m} physical contravariant velocity. Boussinesq eddy viscosity and eddy diffusivity hyperthesis are used to calculate the Reynolds stresses in the momentum equations and the turbulent heat fluxes in energy equation.

Momentum equation

$$\frac{1}{\sqrt{g}}\frac{\partial}{\partial \xi^m}(\sqrt{g}\sqrt{g^{mm}}\,\rho U^{\xi^m}U^i) = -\frac{\partial \xi^m}{\partial x^i}\frac{\partial P}{\partial \xi^m} + \frac{1}{\sqrt{g}}\frac{\partial}{\partial \xi^m}\left(\mu\sqrt{g}\,g^{nn}\frac{\partial U^i}{\partial \xi^n}\right) \tag{3}$$

Table 1 Turbulent model coefficients

$C_{\varepsilon 1}$	$C_{\varepsilon 2}$	σ_k	σ_ε	C_μ
1.44	1.92	1.0	1.3	0.09

Energy equation

$$\frac{\partial}{\partial \xi^m}(\sqrt{g}\sqrt{g^{mm}}\rho U^{\xi^m} T) = \frac{\partial}{\partial \xi^m}\left[\sqrt{g}\, g^{nm}\left(\frac{\mu}{\sigma}+\frac{\mu_t}{\sigma_t}\right)\frac{\partial T}{\partial \xi^n}\right] \tag{4}$$

In order to close the governing equations, following transport equations for the turbulent kinetic energy k and dissipation rate ε are used.

Turbulent kinetic energy equation

$$\frac{1}{\sqrt{g}}\frac{\partial}{\partial \xi^i}(\rho\sqrt{g}\,\widehat{U^i}k) = \frac{1}{\sqrt{g}}\frac{\partial}{\partial \xi^i}\left\{\sqrt{g}\, g^{ij}\left(\mu+\frac{\mu_t}{\sigma_k}\right)\frac{\partial k}{\partial \xi^j}\right\} + P_k - \rho\varepsilon \tag{5}$$

Dissipation rate equation

$$\frac{1}{\sqrt{g}}\frac{\partial}{\partial \xi^i}(\rho\sqrt{g}\,\widehat{U^i}\varepsilon) = \frac{1}{\sqrt{g}}\frac{\partial}{\partial \xi^i}\left\{\sqrt{g}\, g^{ij}\left(\mu+\frac{\mu_t}{\sigma_\varepsilon}\right)\frac{\partial \varepsilon}{\partial \xi^j}\right\} + C_{\varepsilon 1}\rho P_k\frac{\varepsilon}{k} - C_{\varepsilon 2}\frac{\varepsilon^2}{k} \tag{6}$$

The standard values given in Table 1 are adopted for the model constants in equations (5) and (6).

3.2 Numerical analysis

The governing equations were solved numerically by a elliptic finite volume solver. The code solves the 7 dependent variables stored in staggered grid arrangement. In the mean moment equations, the convection terms are approximated by hybrid scheme while in the equations for k, ε and T, the power law differencing scheme is used. The SIMPLE algorithm is used to handle the velocity-pressure linkage. The resulting set of descretized equations are solved semi-implicitely using the tridiagonal matrix algorithm.

Table 2 Dimensions of nuclear reactor bundle

Geometric parameters	Dimensions
Rod diameter (mm)	9.5
Rod pitch (mm)	12.6
S/G pitch (mm)	600
Hydraulic diameter (mm)	11.468
Reynolds number (Re)	10,000
Area of housing (mm)	81×81
Heat flux (kW/m^2)	30

The computational regimes are composed of the spacer grid, mixing vane, housing, and 36 rods. The body fitted coordinate system is employed to match grid lines to the wall boundaries. Inlet flow conditions after mixing vanes are modeled to avoid the difficulty in grid generation around the mixing vanes. Computations are only performed for a quarter of rod bundles, because the flow pattern of the 36 rod bundles are symmetric.

Computational region in streamwise direction is extended to $40\,D_H$, because the turbulent flow is fully developed near the $35\,D_H$ and the grid number are 72×72×25. Table 2 shows the dimensions and flow conditions for the present model of nuclear fuel bundle. Due to the difficulty in grid generation for the flow region around the mixing vane, inlet flow conditions after mixing vanes are modeled as follows.

$$V(W) = \frac{U\tan\alpha\cdot y(z)}{B}, \quad r<B \qquad V(W) = \frac{U\tan\alpha\cdot y(z)B}{r^2}, \quad r\geq B \tag{7}$$

where $r=\sqrt{(y-a)^2+(z-b)^2}$, U is streamwise velocity, V and W is the secondary flow

velocities in y, z directions respectively. And the α with 10°, 20°, 30° is the inclination angle of mixing vane to the streamwise direction.

A general formulation according to the concepts of periodic fully developed flow and heat transfer is developed to accommodate the periodic housing duct with rod bundles. Basically, the test section shown in Fig. 1 can be regarded as a periodically varied cross sectional area in x-direction. Therefore, the physical quantities are decomposed in x-direction. According to Patankar et al.,[9] the pressure P and temperature T of a periodically fully developed flow can be decomposed as

$$P(x, y, z) = -\beta x + P_R(x, y, z) \quad (8)$$

$$T(x, y, z) = \gamma x + T_R(x, y, z) \quad (9)$$

where both the global pressure drop parameter β and the temperature increase parameter γ are constants. The quantities of P_R and T_R identically repeat themselves from spacer grid to spacer grid.

At all the wall boundaries, the no-slip boundary condition, $\varepsilon = 2\mu(\partial\sqrt{k_1}/\partial y_1)^2$ and $k = 0$ are adopted. Constant heat flux are assumed to be applied to the wall of rod bundles. Normal velocities of symmetric lines take.

$$W(z) = -V(y);\ V(y) = W(z) \text{ at } y/L = 0.5 \quad (10)$$

$$W(z) = V(y);\ V(y) = -W(z) \text{ at } z/L = 0.5 \quad (11)$$

4. Results and discussions

The main purpose of the present study is to find out the optimal configuration of mixing vane shape and arrangement pattern which may improve the turbulence thermal efficiency of rod bundles. For this purpose, the weak points of the split mixing vanes should be find out and revised to enhance the turbulent thermal efficiency.

Generally the configurations of spacer grid and mixing vane should be changed to improve the turbulent thermal efficiency of the cooling system. The purpose of spacer grid is to keep a fixed space between the rod bundles and to prevent the vibration of rod bundles. But the mixing vanes attached to the spacer grid increase the heat transfer coefficients of the rod bundle due to its turbulence enhancement effect.

In the present study, computational analysis for the subchannel flow of nuclear reactor cooling system is carried out. The subchannel flows are composed of internal subchannel between 4 rods, wall subchannel flow with single wall and 2 rods, and corner subchannel flow with 2 walls and a single rod. Measuring points for LDV are shown in Fig. 3. About 30,000 data are collected for 20~30 seconds and then averaged. On the dashed lines P1~P7, the measuring points B1~B7 are located.

Figure 4 shows the comparison of decaying processes of secondary motions depicted by the secondary velocity vectors obtained from the computational results for the subchannel flows with split and LSS mixing vanes. Vortex size

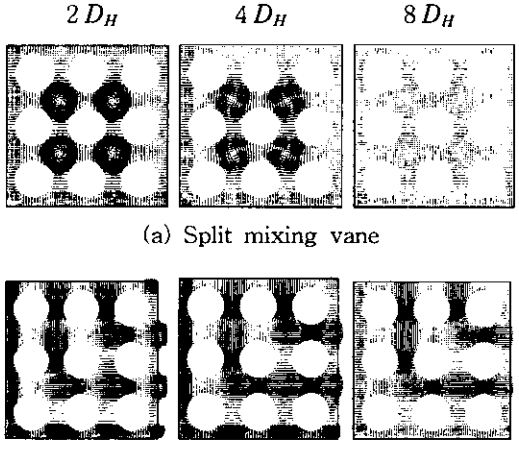

(a) Split mixing vane

(b) LSS mixing vane

Fig. 4 Development of secondary velocity along the streamwise direction for two different mixing vanes.

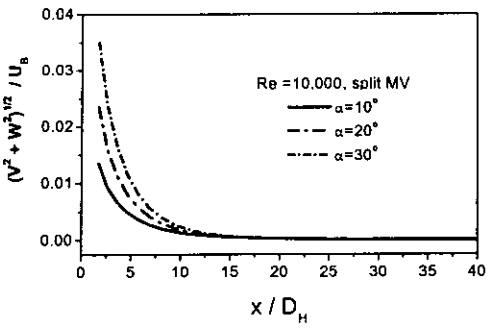

(a) Split mixing vane

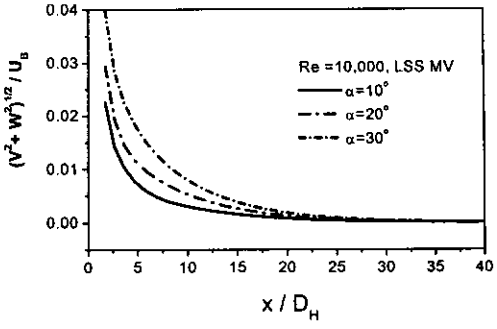

(b) LSS mixing vane

Fig. 5 Variation of cross-sectional averaged secondary flow intensity for the inclination angle of mixing vane.

generated by the mixing vane has dimension of rod diameter but the vortex size generated by the LSS mixing vane has the dimension of spacer grid. In case of split mixing vane, vortices is strongly generated in the subchannel itself, thus the flow mixing between subchannels are negligible. However for the LSS mixing vane, the secondary flows circulate the coolant flow between subchannels thereby generate large scale swirling flow which may cause to generate continually turbulence. At each station, streamwise, secondary and turbulent velocities distributions are measured with every $\Delta x = 0.5\, D_H$ interval up to $32\, D_H$.

Figure 5 shows decaying rate of secondary flow intensity with variation of mixing vane angle for the Reynolds number of 10,000 and the inlet condition of same secondary flow intensity. Secondary flow generated by LSS mixing vane remains up to $25\, D_H$ while $13\, D_H$ only for the split mixing vane.

In Fig. 6, experimental and computational results for the streamwise velocity distributions at the Path 2 and Path 4 are compared. There is a good agreement between the measured and computational velocity distributions at the positions of $2\, D_H$ and $4\, D_H$ of Path 2. But large discrepancies occur between the measured and computational results at the positions of 8, 16 and $32\, D_H$. This phenomenon seems to be occurred due to the strong interaction between the turbulent components near

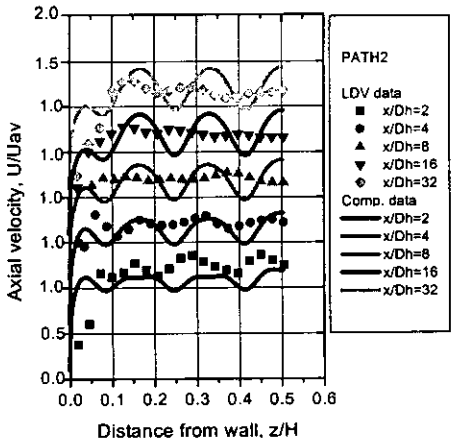

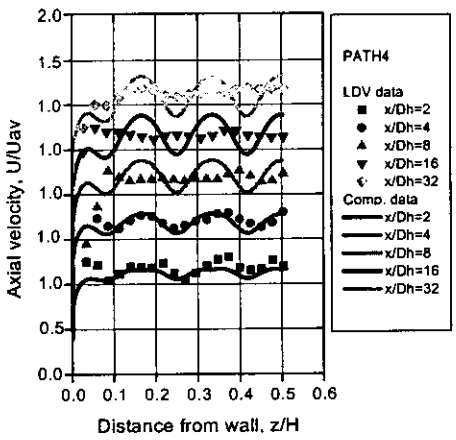

Fig. 6 Developed streamwise velocity.

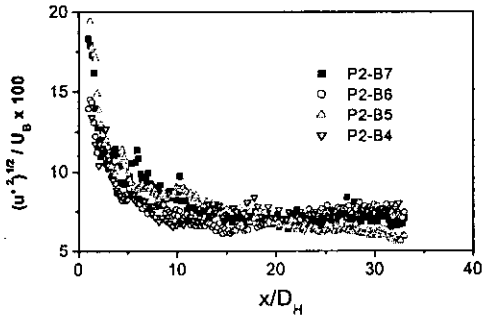

(a) LSS mixing vane (Re=10,000); path 2

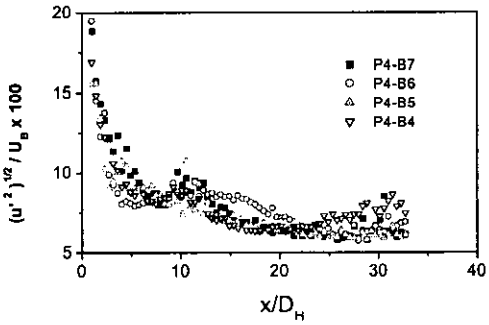

(b) LSS mixing vane (Re=10,000); path 4

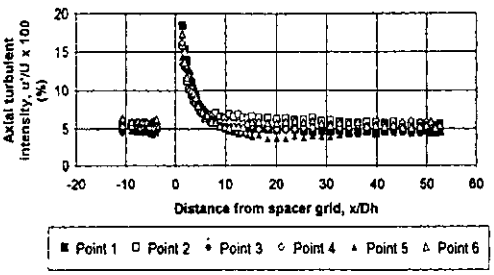

(c) Split mixing vane (Re=50,000)[6]

Fig. 7 Distribution of axial turbulent intensity.

wall and the large scale secondary motion. Development of turbulence in the subchannel flow is mainly dependent on the secondary flow pattern. The discrepancies between the measured and computational velocity distribution are considered to be occurred due to the employment of $k-\varepsilon$ model and insufficient computational grid number. It is generally regarded that the accuracy of $k-\varepsilon$ model could not bear comparison with that of second moment turbulent closures for predicting the strong swirling flow which generate the highly anisotropic turbulent structures.

Figure 7 shows the variations of turbulent intensity measured by LDV with variation of x/D_H. According to the previous research, the enhancement of thermal efficiency by split mixing vane is restricted to a short distance after a spacer grid due to the rapid decay of turbulent intensity.[6] But the Fig. 7 shows that the decays of turbulent intensities for the LSS mixing vane are remarkably delayed in comparison with that of the split mixing vane.

5. Conclusions

In the present study, the effects of the arrangement of mixing vanes on the turbulence enhancement in the cooling system of nuclear reactor are investigated by experimental and computational means. Measured data for the longitudinal variations of streamwise and turbulent velocities are compared with the computational results. From the comparison, the following conclusions are drawn.

(1) The secondary flow generated by the LSS mixing vane remains up to $20\sim25\,D_H$ while $10\sim13\,D_H$ for the split mixing vane.

(2) Turbulence intensities generated by LSS mixing vane decay more slowly after spacer grid than those of split mixing vane. There is a general agreement between the present experimental results and the published ones.

(3) Enhancement of thermal efficiency by the attachment of LSS mixing vanes to the spacer grids is mainly caused by the remarkable reduction of turbulence decaying rate according to the generation of large scale vortex motion in the cross-sectional plane of subchannel after the spacer grid.

Acknowledgements

This study was supported by Korea Electric

Power Corporation (KEPCO Project No. 98-013) of Korea. The authors are grateful to KEPCO.

References

1. Rehme, K., 1973, Nucl. Technol, Vol. 17, pp. 15-23.
2. Rehme, K. and Trippe, G., 1980, 1973, Nucl. Engrg. and Des., Vol. 62, pp. 349-359.
3. Rowe, D. S., Johnson, B. M. and Knudsen, J. G., 1974, Int. J. Heat Transfer, Vol. 17, pp. 407-419.
4. Gu, C. Y., Ji, Wei, Karoutas, Z. and Scholin, B., 3D flow Analyses for Design of Nuclear Fuel Spacer.
5. Shen, Y. F., Cao, Z. D. and Lu, Q. G., 1991, Nucl. Engrg. and Des., Vol. 125, pp. 111-119.
6. Yang, S. K. and Chung, M. K., 1995, 6th Int. Conf. on Laser Anemometery Advances and Applications, South Carolina, USA.
7. Launder, B. E. and Spalding, D. B., 1974, Computer Methods in Applied Mechanics and Engineering, Vol. 3, p. 269.
8. Jayatilleke, C. L. V., 1969, SAE Paper, No. 900254.
9. Patankar, S. V., Liu, C. and Sparow, E. M., 1977, Trans. ASME J. Heat Transfer, Vol. 99, pp. 180-186.